

DYNAMIC THERMAL BEHAVIOUR OF BUILDING USING PHASE CHANGE MATERIALS FOR LATENT HEAT STORAGE

by

Ghouti SELKA^{a*}, Abdel Illah Nabil KORTI^a, and Said ABOUDI^b

^aLaboratory ETAP, University of Tlemcen, Algeria

^bIRTES-M3M, site de Sevenans, UTBM, Belfort Cedex, France

Original scientific paper

DOI: 10.2298/TSCI140311134S

This study presents a two-dimensional model with a real size home composed of two-storey (ground and first floor spaces) separated by a slab, enveloped by a wall with rectangular section containing phase change material in order to minimize energy consumption in the buildings. The main objective of the phase change material-wall system is to decrease the temperature change from outdoor space before it reaches the indoor space during the daytime. The numerical approach uses effective heat capacity C_{eff} model with realistic outdoor climatic conditions of Tlemcen city, Algeria. The numerical results showed that by using phase change material in wall as energy storage components may reduce the room temperature by about 6 to 7 °C of temperature depending on the floor level (first floor spaces or ground floor spaces).

Key words: *latent heat storage, phase change material, numerical simulation, building*

Introduction

One of the most effective means to reduce the energy consumption of the building is to optimize its envelope. Technological solutions have been introduced such as the use of phase change materials (PCM) [1], in active and passive solar buildings which has been subject to considerable interest. The appeal of PCM is that they can smooth daily fluctuations in room temperature by lowering the peak temperatures resulting from extreme external daily temperature changes. The PCM can store heat energy in a latent, as well as sensible fashion, leading to greater heat storage capacity per unit volume than that of conventional materials. As the building trends towards overheating, the PCM melts and absorbs the excess heat due to their phase change from solid to liquid. This heat is only released when the room temperature drops below the specified level and then the liquid PCM returns to a solid state and consequently the room temperature becomes more stable [2, 3].

A numerical investigation to evaluate the performance of heat storage is developed by Heim *et al.* [4]. They evaluate the performance of a PCM-impregnated gypsum board in a test room during different periods. The results obtained with the simulation show that depending on the PCM melting temperature, the wall surface temperature could be about 0.5-1.0 °C lower than in the case with traditional gypsum board. Athienitis [5] investigated gypsum board impregnated with PCM for thermal storage in a passive solar test room. They found that the utilization of the PCM gypsum board may reduce the maximum room temperature up to 4 °C during the daytime. In recent years, a kind of novel shape stabilized phase change material (SSPCM),

* Corresponding author; e-mail: g_selka@yahoo.fr

has been attracting the interests of many searchers [3, 6, 7]. Mushtaq *et al.* [8] have studied the thermal performance of a phase change material based on thermal storage for energy conservation in building with and without PCM for comparison purposes. The melting temperature of PCM chosen is in the range of (36.7-37) °C. Several simulation runs were made for the ambient conditions and for various other parameters of interest. The experiments results demonstrated that heat transfer was reduced by 46.71% compared to the roof without PCM. The use of the wax as latent heat storage in a wallboard was also investigated by Heim [3, 9-12], and it was reported that the latent heat release stabilized the room temperature. Zhang [13] presents the development of a thermally enhanced frame wall that reduces peak air conditioning demand in residential buildings using crystalline paraffin wax, and the cooling load was reduced by 10.8%.

On the other hand, Voelker *et al.* [14] studied the effect of adding micro-encapsulated paraffin to a 30 mm gypsum plaster in a test room. The simulations carried out over one representative week showed a potential reduction of 2 °C in the peak indoor air temperature. Izquierdo-Barrientos *et al.* [15] have studied the integration of a PCM layer into a building wall for diminished the amplitude of the instantaneous heat flux through the wall. The results of the work show that there is no significant reduction in the total heat lost during winter regardless of the wall orientation or PCM transition temperature. In this work, we presented 2-D numerical study using a phase change material to improve thermal performance of a two-storey building in city Tlemcen (Algeria) for one realistic chosen day with known outdoor temperature, solar radiation and wind velocity. A specific paraffin material was placed in a cavity between brick and concrete walls to reduce the room temperature during days. A mathematical model has been developed and the finite volume method is employed for the computation of thermal behavior of the building integrating PCM. A comparison with the results without PCM is made and several simulation runs are conducted with realistic outdoor climatic conditions of Tlemcen city and for the various other parameters of interest.

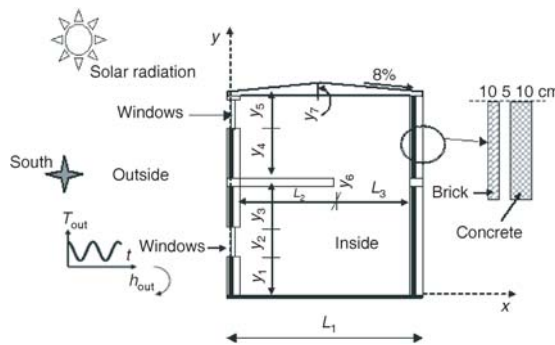


Figure 1. Presentation of the test rooms

during the charging process (sunshine hours), the PCM in the wall change its phase from solid to liquid. During the discharging process (night hours), the PCM changes its phase from liquid to solid by rejecting its heat to the ambient air in the test room. This cycle continues every day. The

Physical problem

The studied solar test room is a building with ground and first floor spaces, separated by a concrete slab, and a concrete pitched roof of 8%, fig. 1. The external walls are composed of concrete and brick. The geometrical properties of the test rooms are represented in tab. 1. A phase change material is provided between the two materials in the form of sandwich. The PCM used is the paraffin. The thermal properties of different materials are presented in tab. 2. In each cycle,

Table 1. Geometrical properties of the test rooms

y_1	y_2	y_3	y_4	y_5	y_6	y_7	L_1	L_2	L_3
1.0 m	1.0 m	0.8 m	1.2 m	1.0 m	0.15 m	0.15 m	3.6 m	2.1 m	1.5 m

boundary condition on the side south of wall and roof is considered to combination the effect of radiation and convection. In order the radiation, the average radiation heat flux available for every one hour in Tlemcen city is used. For convection, the heat transfer coefficient (h) value on the outer surface is calculated based on the pre-
 prevailing velocity of the wind. The boundary condition on the north wall is considered to be natural convection.

Table 2. Thermal properties of materials

Materials	ρ [kgm ⁻³]	λ [Wm ⁻¹ K ⁻¹]	C_p [Jkg ⁻¹ K ⁻¹]
Concrete	2100	1.4	1000
Bric	1920	0.72	835
Glazingk	2500	1.4	720

Table 3. Thermal properties of paraffin

Materials	Appearance (color)	ρ [kgm ⁻³]	λ [Wm ⁻¹ K ⁻¹]	C_p [Jkg ⁻¹ K ⁻¹]	Latent heat [kjkg ⁻¹]	Phase change temperature [°C]
Paraffin	Grey	1019 solid 780 liquid	Eq. (8)	Eq. (7)	240	22-23

Mathematical formulation of the problem

The following assumptions are considered in this study:

- the thermal properties of the brick and concrete are constant, and
- the thermal properties of PCM are variable in each phase (solid and liquid).

The studied system is governed by the following conservative eqs:

In fluid domain: Air

The governing conservation equations for unsteady, incompressible, Newtonian, two-dimensional and laminar flow are given by the expressions:

- continuity

$$\frac{\partial u}{\partial x} + \frac{\partial v}{\partial y} = 0 \tag{1}$$

- x-momentum

$$\rho \left(\frac{\partial u}{\partial t} + u \frac{\partial u}{\partial x} + v \frac{\partial u}{\partial y} \right) = - \frac{\partial p}{\partial x} + \mu \left(\frac{\partial^2 u}{\partial x^2} + \frac{\partial^2 u}{\partial y^2} \right) \tag{2}$$

- y-momentum

$$\rho \left(\frac{\partial v}{\partial t} + u \frac{\partial v}{\partial x} + v \frac{\partial v}{\partial y} \right) = - \frac{\partial p}{\partial y} + \mu \left(\frac{\partial^2 v}{\partial x^2} + \frac{\partial^2 v}{\partial y^2} \right) + \rho g \beta (T - T_0) \tag{3}$$

- energy

$$\rho C_p \left(\frac{\partial T}{\partial t} + u \frac{\partial T}{\partial x} + v \frac{\partial T}{\partial y} \right) = \frac{\partial}{\partial x} \left(\lambda \frac{\partial T}{\partial x} \right) + \frac{\partial}{\partial y} \left(\lambda \frac{\partial T}{\partial y} \right) \tag{4}$$

In solid domains: brick (i = 1), concrete (i = 2), and glass (i = 3)

$$(\rho C_p)_i \frac{\partial T}{\partial t} = \frac{\partial}{\partial x} \left(\lambda_i \frac{\partial T}{\partial x} \right) + \frac{\partial}{\partial y} \left(\lambda_i \frac{\partial T}{\partial y} \right) \quad i=1, 2, 3 \tag{5}$$

In PCM domain

$$\rho C_{\text{eff}} \frac{\partial T}{\partial t} = \frac{\partial}{\partial x} \left(\lambda \frac{\partial T}{\partial x} \right) + \frac{\partial}{\partial y} \left(\lambda \frac{\partial T}{\partial y} \right) \tag{6}$$

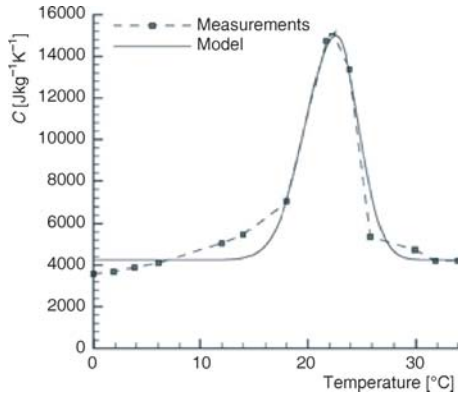


Figure 2. Variation of apparent (effective) heat capacity with temperature [9]

experimental measurements, fig. 2 and eq. (7).

$$C_{eff} = 4250 + 10750 \exp\left(-\frac{295.6 - T}{a}\right) \quad (7)$$

$$\begin{cases} a = 4 & \text{if } T \leq 295.6 \text{ K} \\ a = 3 & \text{if } T > 295.6 \text{ K} \end{cases}$$

The curve corresponding to eq. (7) is plotted in fig. 2. As one can observe, the melting process starts at 15 °C and ends at 28 °C, the peak temperature is 22.6 °C, after which melting is completed quite rapidly. The thermal conductivity varying between 0.18 and 0.22 W/mK and the density is 1019 kg/m³. The thermal conductivity λ is defined by the following relations:

$$\lambda = \begin{cases} \lambda_s & \text{if } T \leq 295.6 \text{ K} \\ \lambda_l & \text{if } T > 295.6 \text{ K} \end{cases} \quad (8)$$

Boundary conditions

The bottom is assumed adiabatic. All walls of the studied rooms are submitted to mixed convection radiation heat transfer with ambient and sky, respectively:

$$Q = h(T - T_a) + \varepsilon\sigma(T^4 - T_{sky}^4) \quad (9)$$

Except at the south wall, the radiation heat flux is added:

$$Q = h(T - T_a) + \varepsilon\sigma(T^4 - T_{sky}^4) + G(t) \quad (10)$$

where $G(t)$ is the solar radiation heat flux according to the typical day of Tlemcen, fig. 3(b), and h – the convection heat transfer coefficient due to wind, recommended by McAdams [16]:

$$h = 5.67 + 3.86v_w \quad (11)$$

where v_w is the wind velocity, fig. 3(c). The Algerian typical day weather of May 12 in Tlemcen (altitude 750 m, latitude 35°28'N, longitude 1°17') is chosen as the outdoor climate data. The hourly

The thermal behaviour of the PCM is based on the apparent capacity method.

Initial conditions

In the fluid domain are: $u = v = 0$, and $T_0 = 288 \text{ K}$.

By making the specific heat of PCM function of temperature, thermal effect of melting and solidification of PCM can be simulated. The geometry of the grid is independent of time, and the liquid/solid interface is tracked by the definition of the specific heat in the governing equations. The specific heat is the rate of change of enthalpy with respect to temperature. The specific heat is the sum of the sensible and latent heats. In our case, the C_{eff} law, proposed by Kuznik [9], is used. It is based on the normal curve of the specific heat adapted by exper-

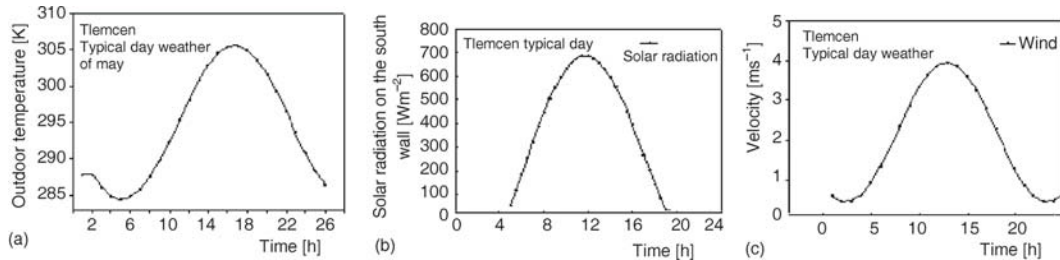


Figure 3. Hourly variation of outdoor air temperature (a), hourly variation of outdoor solar radiation (b), and hourly variation of outdoor wind velocity (c)

variation of outdoor air temperature and solar radiation on the south wall is shown in fig. 3(a). The average outdoor air temperature is 23 °C.

Computational procedure

There are two well-known methods for numerically solving the set of governing equations, the finite volume and the finite element approaches. The commercial CFD software package, FLUENT, which is based on the finite volume approach was used for solving the set of governing equations. FLUENT provides the flexibility in choosing discretization schemes for each governing equation. The discretized equations, along with the initial and boundary conditions, were solved using the segregated solution method to obtain a numerical solution. Using the segregated solver, the conservation of mass and momentum were solved iteratively and the SIMPLE algorithm was used to ensure the momentum and mass conservation, equations in [17]. The convergence criterion was set equal to 10^{-7} for all parameters.

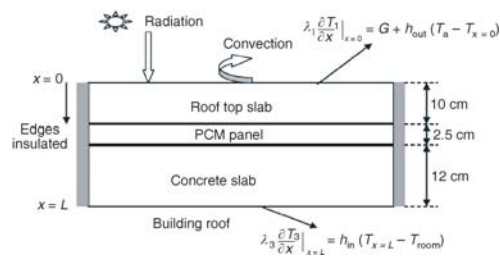


Figure 4. Presentation of the building roof

Experimental validation

The physical system considered is a composite plate filled with PCM placed between the roof top and the concrete slab. During sunshine hours, the PCM changes its phase from solid to liquid. During the night hours, the PCM passes from the liquid to solid phases (solidification) by rejecting its heat to the ambient and to the air inside the room. Initially, the composite plate is maintained at a uniform temperature 27 °C. The boundary conditions and the properties of PCM are given in [18].

Figure 5 shows the experimental and simulated evolutions of the ceiling temperature of the PCM room during 24 h of daytime. There is a good agreement between the measurements and the numerical approach that uses effective heat

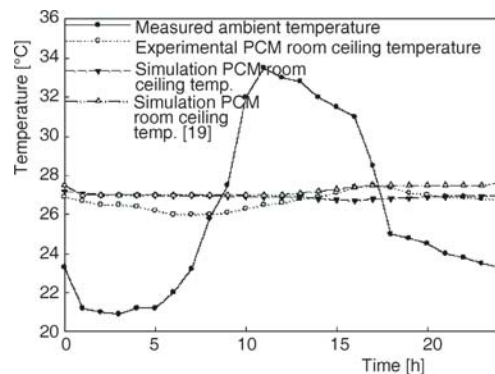


Figure 5. Experimental and simulated temperature of the ceiling in the PCM and non-PCM room

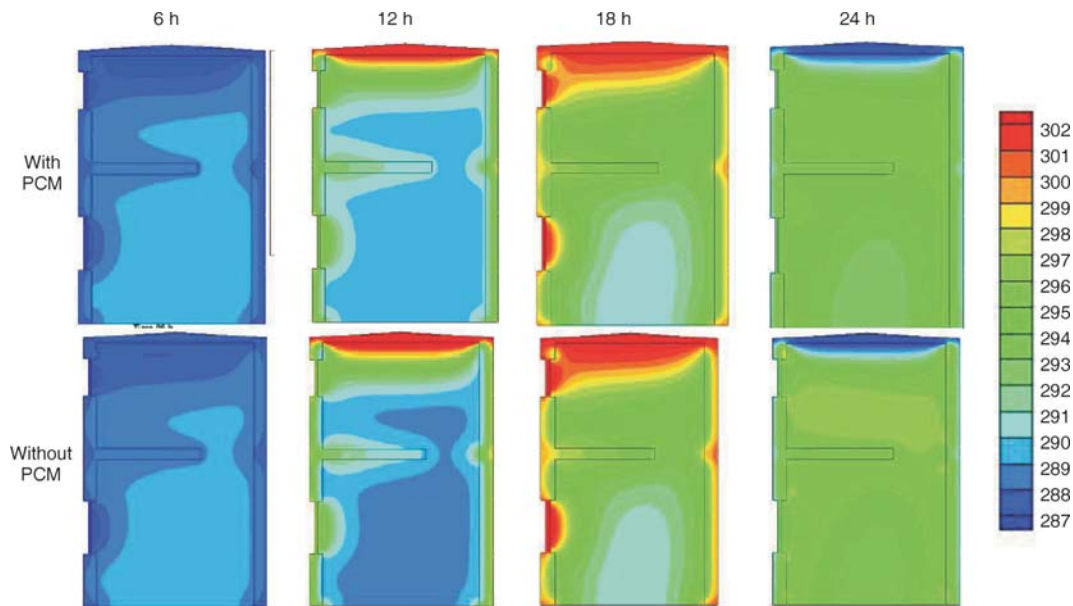


Figure 6. Temperature contour at various hours

capacity model. The maximum temperature difference between the experimental and the numerical obtained curves is about $0.59\text{ }^{\circ}\text{C}$. This shows that the thermal response of the room is correctly reproduced by the thermal model.

Before the numerical analysis, the grid-independency of the test rooms system was simply checked using a different number of grids. The system was finally divided into 8599 cells with 9188 nodes in consideration of grid-independency and calculating efficiency.

Results and discussions

Figure 6 shows the evolution of the temperature field inside the test room at 06:00, 12:00, 18:00, and 24:00 hours. The outdoor temperature varies from 286 K to 306 K. We can notice that the test room's maximum temperature vary *vs.* time. In fact, during solar radiation, at 12:00 for example, the test room becomes warmer. The temperature is higher near the roof because of the low thermal conductivity of the concrete and the absence of insulator. A vertical thermal gradient is also observed near the top and advance down. The evolution of the temperature is more important in the south wall than in the north wall because the north wall receive less solar radiation. At 18:00, despite the outdoor temperature and solar radiation decrease, the room temperature continues to increase. This phenomenon is due to the sensible heat and latent heat stored respectively by test room walls and by PCM. At 24:00, the room temperature remains constant at approximately 297 K. It also records the start of cooling at the roof due the heat energy released by PCM. Therefore, for the first floor space, there is a significant influence of the roof thermal conductivity temperature thus the roof materials should be carefully chosen to provide air temperature comfort. However, the air temperature on the ground floor spaces is acceptable (297 K).

Figure 7 shows the evolution of the air temperature during four days. The room temperature is stabilized between 292 K and 295.7 K at 24:00 of the days. The temperature difference

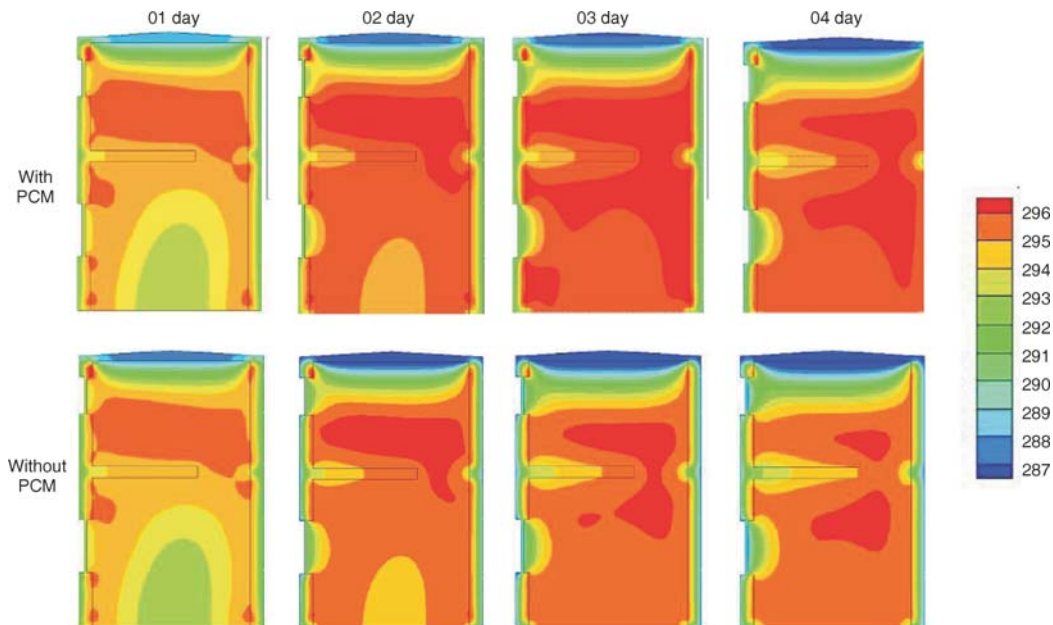


Figure 7. Evolution of the air temperature

between the ground and the first floor spaces do not exceed 3.2 K (3.16 K an empty wall cavity). It can be seen that the maximal temperature reached is 295.65 K (295.36 K an empty wall cavity) in the higher level after 24 h and 296.35 K (296.43 K an empty wall cavity) after 48 h, respectively. In the lower level, the maximal temperature reached is 294.11 K (293.88 K an empty wall cavity) after 24 h and 295.68 K (296.03 K an empty wall cavity) after 48 h, respectively. The PCM can reduce considerably the room temperature. The PCM composite walls allow enhancing the thermal comfort of the test room under these conditions. The maximum air temperature is decreased by about 6.8 K and the minimum increased by about 3.1 K. Another notable effect is the natural convection enhancement allowing to have a better mixing concerning the air in the test room and decreasing the temperature gradient.

It is interesting to note that a thermal gradient exists in the first floor spaces (a difference maximum of 4.9 K for the temperature between the bottom and the top). This is mainly due to higher natural convection effects because of the temperature of roof. This affects the thermal comfort in upper room.

Figure 8 illustrates the temperature profiles at different times (6, 12, 18, and 24 h o'clock) inside space the room ($x = 1.75$ m). At 06 h o'clock, we note the beginning of cooling in the test room and at 12 h, the room temperature in the first floor spaces reached 293 K due to the intense solar radiation. However, the room temperature in the ground floor spaces is lower than 289 K due the separation slab.

At time 18 h o'clock, we see the increase of room temperature in the ground floor spaces at approximately 293 K, and the room temperature in the first floor spaces begins to decrease and indicates that the heat gain is effectively absorbing through melting/solidification process.

At time 24 h o'clock, the convection heat exchange is strongly reduced between the outdoor and the inside spaces. The air temperature of the first floor spaces is lower (begin internal

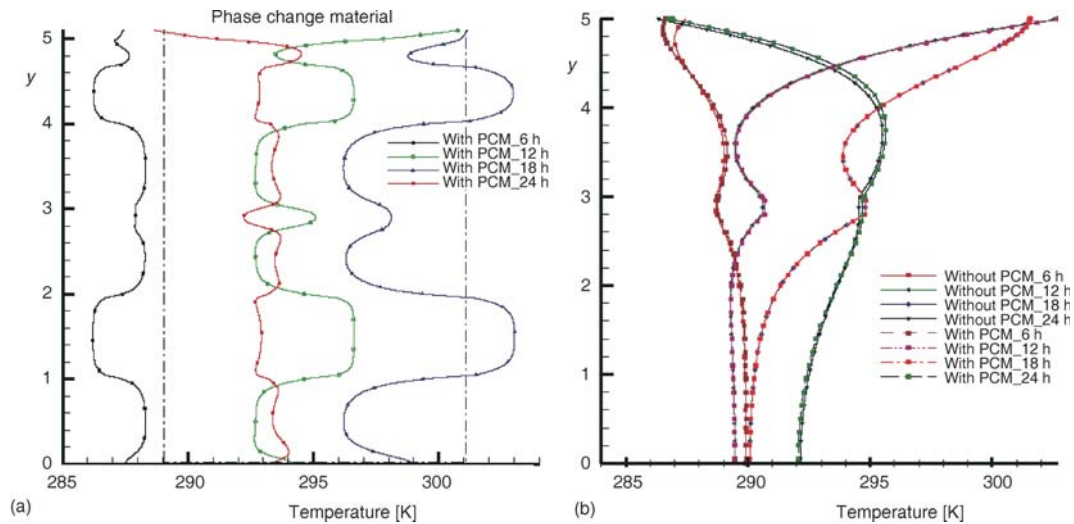


Figure 8. Temperature profiles at different times at (a) $x = 0.13$ m, and (b) $x = 1.75$ m

cooling) than that the room temperature of the ground floor spaces. To compare the performances storing energy savings, a numerical simulation with the PCM between the walls (case 1) is compared to a simulation without PCM (an empty wall cavity) case 2. Figures 8 show the room temperature evolutions of the test room ($x = 1.75$ m) during the four periods of day at 6:00, 12:00, 18:00, and 24:00.

At 6:00, the room temperature inside the test room with the PCM material is higher compared to that without PCM. A lower conductivity of air allows the better insulation compared to the PCM. At this time, the temperature of the PCM is lower than 288 K and the PCM is completely solid. At 12:00, the room temperature difference of the test room with and without PCM is lower than at 6:00. The PCM temperature is in the phase change region and become partially liquid. The PCM begins to absorb the latent heat and the insulation become better than the air. At 18:00, the room temperature is almost the same with and without PCM. At 24:00, the

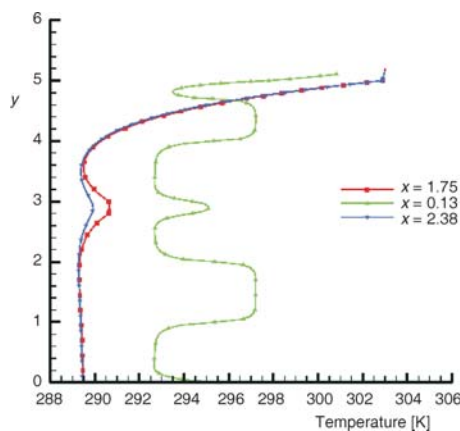


Figure 9. Evolutions of temperatures a long y -axis at $x = 0.13$, 1.75 , and 2.38

room temperature of the test room with PCM is lower to that with empty wall. By reason the PCM temperature decrease and the liberation of the latent heat. So, the PCM acts as a thermal energy accumulator and regulate more perfectly the room temperature that the air insulation.

Figure 9 illustrates the evolution of temperatures at different positions of the south ($x = 0.13$ m), north ($x = 2.38$ m) PCM walls and inside space of the test room ($x = 1.75$ m). The temperature profile of the south PCM wall presents four peaks due to the presence of the thermal bridging (glazing and slab concrete). We note also that the south wall temperature is higher than the room and the north wall temperatures due to the solar radiation incident.

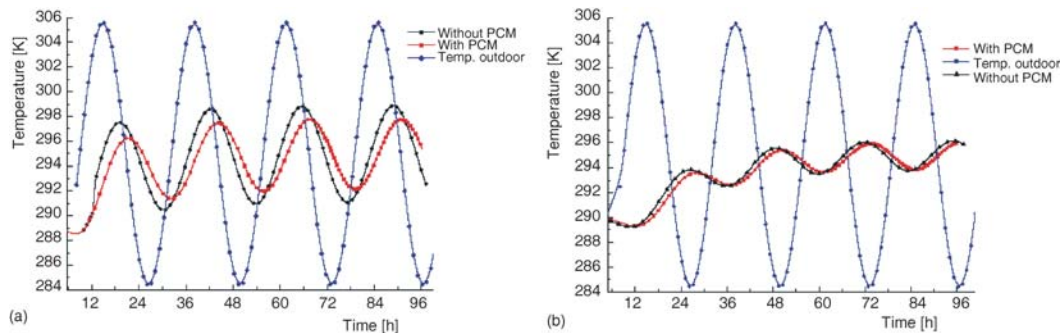


Figure 10. Temperature evolutions at first floor spaces and outdoor spaces (a) and temperature evolutions at ground floor spaces, and outdoor spaces (b)

It is interesting to perceive that the room temperature profile evolution in the north wall is more stable than the south wall temperature. Then, the south wall presents a thermal energy accumulator. We can notice in the spaces ground floor the temperature fluctuations are reduced about 4.5 K in the south wall and 0.5 K in the north wall. However, in the first floor spaces, the phenomena is inverted. In fact, the temperatures fluctuations at the north wall (13 K) are higher than the south wall (8.5 K).

Figure 10 presents temperature evolutions at ground, first floor and outdoor spaces during four days (96 h) with and without PCM (empty cavity). We can see that the room temperature variation peak of first floor spaces is higher than the room temperature variation of ground floor spaces due to the absence of insulation in the roof. To reduce the room temperatures peak in the first floor spaces it is recommended to place the insulation in the roof. However, a time shift is about 6 hours (with PCM) and 4 hours (with empty cavity) between the outdoor and the inside room temperatures in the first floor spaces. This time shift is about 12 hours (with PCM) and 10 hours (with empty cavity) in the ground floor spaces. The time shift in the ground floor spaces is lower than the first floor spaces because the non insulation of the roof and the presence of the slab separation. The time shift with PCM is higher than with empty cavity. This indicates clearly the presence of phase change and the associated heat storage amplitudes.

A important average attenuation between the outdoor spaces and room temperature amplitudes is approximately 8 K (with PCM) and 6.8 K (with empty cavity) in first floor spaces and 9.5 K (with PCM) and 9 K (with empty cavity) in ground floor spaces. The important temperature amplitudes recorded in the first floor spaces shows clearly the good insulation of the PCM compared to the empty cavity. The temperature evolution of the ground floor spaces shows a visible constant level during the first instants (about 1 or 2 hours) corresponding to the heat storage due to the phase change material. The maximum temperature is about 306 K for outdoor spaces, 297.8 K (with PCM) and 299 K (with empty cavity) for first floor spaces and 296.1 K (with PCM) and 296.5 K (with empty cavity) for ground floor spaces. However, the temperature difference between ground and first floor spaces is about 1.2 K (with PCM) and 2.5 K (with empty cavity). This proves clearly that the incorporation of PCM in walls allows us to smooth out fluctuations in the room temperature, reducing daily energy consumption corresponding to a drop in temperature of about 6 to 7 K with respect the outdoor temperature.

Conclusions

A thermal performance, of phase change material (PCM) integrated in wall, has been numerically evaluated in a passive solar building in Tlemcen (West of Algeria) with an effective

heat capacity C_{eff} model. In this study, a real size home composed of two-storey (ground and first floor spaces) was investigated in typical day weather. From the foregone discussion, we have found that the numerical results showed that using PCM in wall as energy storage components may reduce of the room temperature about 6 to 7 K of temperature depending the floor level (first floor spaces or ground floor spaces). This shows that the application of PCM significantly reduces variations of the inside temperature of the test room by absorbing heat during daytime and releasing it at night. It is interesting to note that the excess heat is stored in the PCM. The PCM layer can work as a semi-thermal insulator when solar radiations are not available.

Secondly, the results show that, in the present conditions, typically in Tlemcen, the average room temperature is about 297 K corresponding to the human comfort in buildings. On the whole, the PCM tested enable to maintain the room air temperature within the comfort zone by decreasing the maximum air temperature of the room to a maximum value of 296 K in ground floor spaces and 297.6 K in first floor spaces. This improved thermal comfort is more important if we place a PCM layer in the roof of the test room. The last interesting observation concerns the thermal gradient of the test room which exists in first floor spaces but not in the ground floor spaces for the reason that in the ground floor spaces, the PCM wall insulation is enhanced with slab separation.

The other factor is the time lag is about 6 hours (with PCM) and 4 hours (with empty cavity) between the outdoor and the room temperatures in the first floor spaces. This time lag is about 12 hours (with PCM) and 10 hours (with empty cavity) in the ground floor spaces. The attenuation effect of the mean interior test room temperature by integrated of PCM wall is very obvious, and the time lag effect during the heating period is noticed in each level. The simulation results showed that the additional thermal mass of the PCM can reduce daily room temperature fluctuation by up to 8 K (6.8 K with empty cavity) in first floor spaces and 9.5 K (with PCM) and 9 K (with empty cavity) in ground floor spaces.

Nomenclature

C_{eff}	– effective heat capacity, [$\text{kJkg}^{-1}\text{K}^{-1}$]
G	– radiation flux, [Wm^{-2}]
h	– heat transfer coefficient, [$\text{Wm}^{-2}\text{K}^{-1}$]
h_{in}	– inside heat transfer coefficient, [$\text{Wm}^{-2}\text{K}^{-1}$]
h_{out}	– outside heat transfer coefficient, [$\text{Wm}^{-2}\text{K}^{-1}$]
S	– area, [m^2]
T	– temperature, [K]
T_a	– ambient temperature, [K]
u, v	– velocity components in x- and y-direction, [ms^{-1}]

T_{sky}	– sky temperature, [K]
t	– time, [s]
v_w	– wind velocity, [ms^{-1}]
x, y	– Cartesian co-ordinates, [m]

Greek symbols

ε	– emissivity, [–]
λ	– thermal conductivity, [$\text{Wm}^{-1}\text{K}^{-1}$]
ρ	– density, [kgm^{-3}]
σ	– Stefan-Boltzmann constant, [–]

References

- [1] Feldman, D., et al., Energy Storage Composite with an Organic PCM, *Solar Energy Materials*, 18 (1989), 6, pp. 333-341
- [2] Hadjieva, M., et al., Composite Salt Hydrate Concrete System for Building Storage, *Renewable Energy*, 19 (2000), 1-2, pp. 111-115
- [3] Inaba, H., Tu, P., Evaluation of Thermophysical Characteristics on Shape-Stabilized Paraffin as a Solid-Liquid Phase Change Material, *Heat and Mass Transfer*, 32 (1997), 4, pp. 307-312
- [4] Heim, D., Clarke, J. A., Numerical Modelling and Thermal Simulation of PCM Gypsum Composites with ESP-r., *Energy and Buildings*, 36 (2004), 8, pp.795-805
- [5] Athienitis, A., et al., Investigation of the Thermal Performance of a Passive Solar Test-Room with Wall Latent Heat Storage, *Building and Environment*, 32 (1997), 5, pp. 405-410

- [6] Xiao, M., *et al.*, Preparation and Performance of Shape Stabilized Phase Change Thermal Storage Materials with High Thermal Conductivity, *Energy Conversion Management*, 43 (2002), 1, pp. 103-108
- [7] Zhang, Y., *et al.*, Influence of Additives on Thermal Conductivity of Shape-Stabilized Phase Change Material, *Solar Energy Materials & Solar Cells*, 90 (2005), 11, pp. 1692-1702
- [8] Mushtaq, T., *et al.*, Experimental and Numerical Study of Thermal Performance of a Building Roof including Phase Change Material (PCM) for Thermal Management, *Global Advanced Research Journals*, 2 (2013), 8, pp. 231-242
- [9] Kuznik, F., *et al.*, Energetic Efficiency of Room Wall Containing PCM Wallboard: A Full-Scale Experimental Investigation, *Energy and Buildings*, 40 (2008), 2, pp. 148-156
- [10] Zhou, G., *et al.*, Thermal Analysis of a Direct-Gain Room with Shape-Stabilized PCM Plates, *Renewable Energy*, 33 (2008), 6, pp. 1228-1236
- [11] Tayeb, A. M., A Simulation Model for a Phase Change Energy Storage System: Experimental and Verification, *Energy Convers Manage*, 34 (1993), 4, pp. 243-250
- [12] Esen, M., Durmu, A., Geometric Design of Solar-Aided Latent Heat Store Depending on Various Parameters and Phase Change Materials, *Solar Energy*, 62 (1998), 1, pp. 19-28
- [13] Zhang, M., *et al.*, Development of a Thermally Enhanced Frame Wall with Phase Change Material for On-Peak Air Conditioning Demand Reduction and Energy Saving in Residential Building, *Int. J. Energy Research*, 29 (2005), 9, pp. 795-809
- [14] Voelker, C., *et al.*, Temperature Reduction Due to the Application of Phase Change Materials, *Energy and Buildings*, 40 (2008), 5, pp. 937-944
- [15] Izquierdo-Barrientos, M. A., *et al.*, A Numerical Study of External Building Walls Containing Phase Change Materials (PCM), *Applied Thermal Engineering*, 47 (2012), Dec., pp. 73-85
- [16] McAdams, W. H., *Heat Transmission*, 3rd ed., McGraw-Hill, New York, USA, 1954
- [17] Ismail, K. A. R., Castro, J. N. C., PCM Thermal Insulation in Buildings, *Int. Journal of Energy Research*, 21 (1997), 14, pp. 1281-1296
- [18] Pasupathy, A., *et al.*, Experimental Investigation and Numerical Simulation Analysis on the thermal Performance of a Building Roof Incorporating Phase Change Material (PCM) for Thermal Management, *Applied Thermal Engineering*, 28 (2008), 5-6, pp. 556-565